Wind Energ. Sci. Discuss., https://doi.org/10.5194/wes-2018-63
Manuscript under review for journal Wind Energ. Sci.
Discussion started: 4 October 2018

WIND ENERGY SCIENCE DISCUSSIONS

Comparison between upwind and downwind designs of a 10 MW wind turbine rotor

Pietro Bortolotti, Abhinav Kapila, and Carlo L. Bottasso
Wind Energy Institute, Technische Universität München, D-85748 Garching, Germany
Correspondence to: Carlo L. Bottasso (carlo.bottasso@tum.de)

Abstract. The size of wind turbines has been steadily growing in the pursuit of a lower cost of energy by an increased wind capture. In this trend, the vast majority of wind turbine rotors has been designed based on the conventional three-bladed upwind concept. This paper aims at assessing the optimality of this configuration with respect to a three-bladed downwind design, with and without an actively controlled variable coning used to reduce the cantilever loading of the blades. A 10 MW wind turbine is used for the comparison of the various design solutions, which are obtained by an automated comprehensive aerostructural design tool. Results show that, for this turbine size, downwind rotors lead to blade mass and cost reductions of 6% and 2%, respectively, compared to equivalent upwind configurations. Due to a more favorable rotor attitude, the annual energy production of downwind rotors may also slightly increase in complex terrain conditions characterized by a wind upflow, leading to an overall reduction in the cost of energy. However, in more standard operating conditions, upwind rotors return the lowest cost of energy. Finally, active coning is effective in alleviating loads by reducing both blade mass and cost, but these potential benefits are negated by an increased system complexity and reduced energy production. In summary, a conventional design appears difficult to beat even at these turbine sizes, although a downwind non-aligned configuration might result in an interesting alternative.

1 Introduction

The size of wind turbines in terms of both rotor diameter and nameplate power has been dramatically increasing over the last few decades. The key driver behind this spectacular growth has been the reduction in levelized cost of energy (CoE), which typically benefits from an increase in energy capture. The trend is expected to continue as more countries promote new offshore installations and onshore wind increases its presence in regions of low average wind speeds. In addition, in countries characterized by a high penetration of wind power such as Denmark and Germany, the structure of the electricity market tends to favor larger rotor sizes. In fact, the price of electricity in these markets is increasingly correlated with the availability of wind power. At times when wind power is abundant, electric grids may experience an excess of power generation, which in turn leads spot market prices to markedly drop (Badyda and Dylik, 2017), ultimately reducing the importance of power production in high winds.

The growth in rotor diameters is however pushing the limits of conventional wind turbine configurations. For example, one especially important design driver of very long blades is the minimum clearance between tip and tower to prevent strikes.

In fact, the design of large upwind rotors is typically driven by tip-clearance requirements (Bortolotti et al., 2016, 2018). To meet this constraint, designers are increasingly adopting a combination of thick airfoils and high-modulus composites to increase the out-of-plane stiffness of the blades. Together with an increase in rotor cone and nacelle uptilt angles, these design choices help satisfying the tower clearance constraint. Nonetheless, achieving CoE reductions by upscaling conventional upwind configurations is an increasingly challenging task.

In this scenario, the recent literature suggests that downwind rotor configurations may offer the opportunity to generate lower CoE values compared to traditional upwind ones (Frau et al., 2015). Cost reductions could be obtained in downwind configurations thanks to lighter and more flexible blades, made possible by a relaxed tower clearance constraint. In addition, an increased AEP could be generated by reduced cone and uptilt angles, as well as by a favourable blockage effect generated ① by the nacelle. In sites characterized by upflow angles, such as hills and ridges, the uptilt angle improves the alignment of the rotor with the incoming wind in the downwind case, while it has the opposite effect in the upwind one. Lastly, downwind rotors could, at least in principle, be designed without an active yaw system (Kress et al., 2015a).

Clearly, these benefits would not come for free, and downwind rotors struggle against a major disadvantage, namely an increased tower shadow effect (Reiso, 2013). This results into two main negative effects compared to equivalent upwind designs. First, fatigue loading typically increases due to a higher one-per-revolution harmonic blade excitation (Manwell et al., 2009; Kress et al., 2015b). Secondly, higher noise emissions are generated due to the blade interference with the tower wake, especially in the low frequency range of the noise spectrum (Madsen et al., 2007). These two aspects have been especially important for early onshore machines and, as a result, most modern designs worldwide adopt the upwind configuration. One notable exception to this situation is represented by the downwind machines developed by Hitachi Ltd. and installed in Japan (Kress et al., 2015b).

An additional potential advantage of downwind rotors is the possibility of achieving the so called "load alignment" along the blades, a novel concept proposed and investigated in Ichter et al. (2016); Loth et al. (2017); Noyes et al. (2018). Load alignment may be seen as bio-inspired by palm trees, which sustain storms by bending downwind and aligning their leaves in the wind direction, which has the effect of turning cantilever loads into tensile ones. In Ichter et al. (2016); Loth et al. (2017); Noyes et al. (2018) this concept is investigated by designing a 13.2 MW two-bladed downwind rotor, which exhibits a decreased CoE in comparison to an equivalent upwind three-bladed configuration. This claim is supported by reduced out-of-plane fatigue and ultimate loads that lead to a reduction of the blade mass.

Goal of this work is the comparison of three-bladed upwind rotor configurations with three-bladed downwind designs, including load alignment. The present work does not consider the case of teetering two-bladed rotors. The novelty of the present investigation resides in the fact that, differently from the existing literature, each wind turbine design is subjected to a detailed aerostructural optimization to minimize its CoE. The comprehensive design procedures used here account for all necessary design constraints and consider the various multi-disciplinary couplings of the problem, which are necessary to identify CoE-optimal constraint-satisfying solutions. This is achieved by balancing turbine capital cost and annual energy production (AEP). Examples of publicly available design frameworks include `HAWTOpt2` (Zahle et al., 2016), `WISDEM` (Dykes et al., 2014) and `Cp-Max` (Bortolotti et al., 2016, 2018), the latter being used for the present investigation.

Wind Energ. Sci. Discuss., https://doi.org/10.5194/wes-2018-63
Manuscript under review for journal Wind Energ. Sci.
Discussion started: 4 October 2018

The design optimization procedures are driven by the combination of two cost models. A first model developed at Sandia National Laboratories (Johans and Griffith, 2013) is used to estimate the blade cost. This model overcomes the use of simplified relationship between blade mass or blade length versus blade cost, and it accounts for material, equipment and labor costs. CoE is estimated by the cost model developed within the INNWIND.EU project (INNWIND.EU, Deliverable 1.23 , 2014). This second cost model is especially focused on next-generation offshore wind turbine designs.

The presentation is structured as follows. Section 2 presents the aeroservoelastic simulation models used in the study, the load alignment concept and a short summary of the aerostructural design procedures. Then, Sect. 3 discusses the wind turbine configuration used as baseline and the novel downwind designs, which are compared in terms of loads, performance and costs. The study is closed in Sect. 4, where the main conclusions of the study are summarized.

2 Modeling, simulation and design

This work is concerned with the evaluation of design configurations of wind turbines. This activity is supported by the wind turbine design framework `Cp-Max`, which uses aeroservoelastic models implemented with the wind turbine simulator `Cp-Lambda` coupled to a model-based controller, which are described in Sect. 2.1 and 2.2, respectively. This background information is followed by Sect. 2.3, where the load alignment design concept is reviewed. Finally, Sect. 2.4 briefly recalls the design procedures implemented in `Cp-Max`.

2.1 Aeroelasticity

The aeroelastic behavior of the various wind turbine design configurations is computed in this work with the aeroservoelastic simulator `Cp-Lambda` (Code for Performance, Loads and Aeroelasticity by Multi-Body Dynamic Analysis). `Cp-Lambda` implements a multi-body formulation for flexible systems with general topologies and features a library of elements, which includes rigid bodies, non-linear flexible elements, joints, actuators and aerodynamic models (Bottasso et al., 2006; Bauchau, 2011). Sensor and control elements enable the implementation of generic control laws. The multi-body index-3 formulation is expressed in terms of Cartesian coordinates, while constraints are enforced by scaled Lagrange multipliers. In this study, the rotor blades and the tower are modeled by non-linear geometrically-exact shear and torsion-deformable beam models. Fully populated stiffness matrices account for couplings generated by anisotropic composite materials. Flexible components are discretized in space, leading to a system of differential algebraic equations in the time domain.

For aerodynamics, the blade characteristics are defined by lifting lines, which include the spanwise chord and twist distributions as well as sectional aerodynamic coefficients, given in tabular form and parameterized in terms of Reynolds number. The calculation of aerodynamic loads is performed at selected points, called air stations, along each lifting line. Each air station is rigidly connected to an associated beam cross-section, and moves with it. As a consequence, the local airflow kinematics at each air station include the contributions due to blade movement and deformation. In addition, the effects of the wake are modeled by a classical Blade-Element Momentum (BEM) model based on annular stream tube theory with wake swirl and unsteady corrections (Hansen, 2008), or by the dynamic inflow model of Pitt and Peters (1981); Peters and He (1995). The aerodynamic description is completed by root and blade tip losses, unsteady aerodynamic corrections, dynamic stall, 3D blade root delayed stall and upwind and downwind rotor-tower interference models.

A parameterized model of the blade structure is defined by choosing a number of control stations. At each section of interest, airfoils, blade topology, composite mechanical properties and the geometry of the cross section structural members are given, and the cross sectional solver `ANBA` is used to produce the associated six-by-six stiffness matrix and sectional blade properties. In turn, these properties are used to define the corresponding beams in the `Cp-Lambda` model.

2.2 Model based controller

The virtual wind turbines developed in this study are governed over their entire operating range by a controller interfaced with `Cp-Lambda` through external dynamic libraries. A supervisory unit manages the machine behavior by switching among different operating states and handling emergencies. Pitch and torque are handled by suitable controllers operating in closed-loop with the machine on the basis of data supplied by sensor models. All wind turbine models developed in the current study use the linear quadratic regulator (LQR) described in Bottasso et al. (2012). This model-based formulation allows for a straightforward update of the control laws during design, as its underlying reduced-order model can be readily updated whenever the wind turbine parameters change, thereby automatically producing new sets of gains that work in combination with the new design. While probably not superior to other classical pitch-torque controllers used in industrial practice, this method is found to be useful in this research context as it allows for an automatic tuning of the control laws throughout the design process.

The LQR controller is synthesized by means of simulations run in steady wind conditions to evaluate the aerodynamic performance of the machine for a three-dimensional grid of tip speed ratios λ, blade pitch angles β and wind speeds V. These simulations take into account the aeroelastic effects of the flexible bodies of the entire wind turbine model and include the computation of aerodynamic, inertial and gravitational loads. The aerodynamic performance is evaluated by extracting internal forces at the hub, which yield the thrust force and shaft torque. By non-dimensionalizing these values, one obtains the thrust $\mathrm{C_T}$ and power $\mathrm{C_P}$ coefficients, as functions of λ, β and V, which are stored in look-up tables. Based on the $\mathrm{C_P}$ tables, the regulation trajectory of the machine is computed, defining the control parameters (pitch, rotational speed and torque) for regions II and III, defined as the operating regions between cut-in wind speed V_{in} and rated wind speed V_{r}, and between V_{r} and cut-out wind speed V_{out}, respectively (Bottasso et al., 2012). In region II, $\mathrm{C_P}$ is maximized, while in region III power is held constant. In addition, the rotor is regulated to comply with a possible limit on the maximum blade tip speed, which may result in the appearance of a transition region II½ in between the partial and full loading regimes.

2.3 Load aligned rotor

The concept of load alignment for wind turbine rotors has been introduced and developed in Ichter et al. (2016); Loth et al. (2017); Noyes et al. (2018). The idea consists of designing highly pre-bent blades to align the resultant of the various forces acting on the blades with their axis. The goal of such alignment is to convert out-of-plane cantilever forces into tensile ones, which can be resisted by a lighter weight structure.

Wind Energ. Sci. Discuss., https://doi.org/10.5194/wes-2018-63
Manuscript under review for journal Wind Energ. Sci.
Discussion started: 4 October 2018

The primary forces acting on a wind turbine rotor are the thrust force F_t, centrifugal force F_c and gravitational force F_g. Since F_t greatly depends on the wind speed and F_c on the rotational speed, which in turn depends on the wind speed as well, the force resultant changes magnitude and direction over time. An exact load alignment can then be achieved only by a truly morphing blade that adjusts its out-of-plane shape based on wind speed. In this study, the prebent shape of the blade is instead assumed to be frozen, while an out-of-plane load alignment at blade root is sought by means of three flap hinges and three corresponding actuators. Goal of hinges and actuators is to actively control the cone angle γ of each blade. Figure 1 shows a schematic view of this concept.

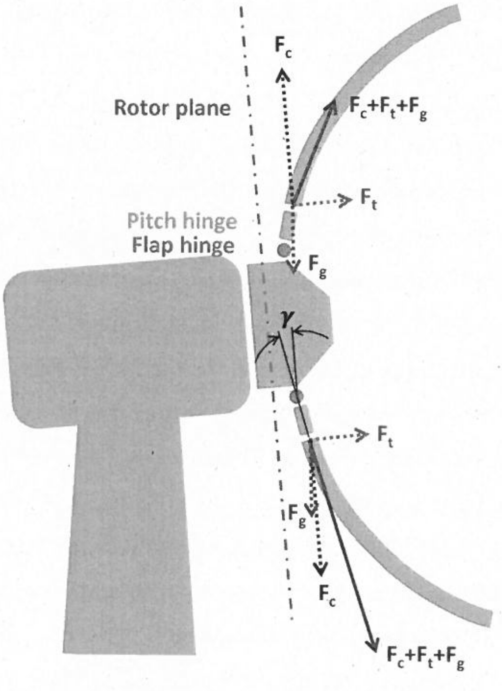

Figure 1. Schematic view of the active load alignment concept.

The resultant of the three forces F_t, F_c and F_g does not only depend on wind speed, but also changes its direction with the azimuthal position of the blade. This change is caused by the periodic variation of the gravitational loading F_g acting on the rotating blade, and by the atmospheric wind shear influencing F_t. As a result, an exact load alignment at blade root can only be achieved by an individual control of the angle γ for each one of the blades. This would however require a flap actuator control rate of several degrees per second. In addition, individual flapping of the blades would break the rotor axial symmetry, generating major rotor mass imbalances. Because of these reasons, an average (collective) γ is used for the three blades, which is changed based on wind speed. A maximum value is set for the blade root out-of-plane moments across one whole rotor revolution. When this threshold value is exceeded, the rotor blades are collectively coned by an angle γ. The coning value is chosen based on a 30-second moving average of the wind speed, which removes fast fluctuations and aims at identifying

Wind Energ. Sci. Discuss., https://doi.org/10.5194/wes-2018-63
Manuscript under review for journal Wind Energ. Sci.
Discussion started: 4 October 2018

the current mean operating condition. To avoid inaccuracies of the nacelle anemometer, a rotor-equivalent wind speed may be obtained by a suitable estimator (Soltani et al., 2013).

2.4 Blade aerostructural design optimization

`Cp-Max` implements wind turbine design methods that integrate a blade aerodynamic optimization with a blade and tower structural optimization, within an overall turbine optimization procedure. The optimization loops are structured following a nested architecture and the overall design goal is the minimization of the CoE. In this study, only the aerodynamic and the structural optimization loops of the blade are used, while the tower is held frozen. For a more complete overview of the design methodologies implemented in `Cp-Max`, interested readers can refer to Bortolotti et al. (2016) and references therein.

The aerodynamic optimization loop is used here to compute an optimal twist distribution for all designed blades. However, the planform shape of all blades was kept the same of the baseline design. Twist is parameterized along the blade span at a number of stations. In each station, an optimization variable is defined, corresponding to an additive gain added to the local twist. The actual twist distribution is reconstructed by means of Piecewise Cubic Hermite Interpolating Polynomial (PCHIP) splines. The merit figure of the aerodynamic optimization is the maximization of AEP, while linear and non-linear constraints are appended to the problem to specify all necessary design requirements and desired features.

The structural optimization aims at the sizing of the blade inner structure for a given outer blade shape. The optimization consists of an iterative loop, beginning with the calculation of the regulation trajectory and the synthesis of the LQR controller gains, which are updated based on the current wind turbine design (Bottasso et al., 2012). Next, a load computation step is performed where a list of design load cases (DLCs) is run. The post-processed results of these analyses are used to compute the load envelopes at a number of verification stations along the three blades. The rainflow counting required to estimate fatigue damage is also performed here. Given these inputs, the actual structural sizing is computed by means of a sequential quadratic programming (SQP) algorithm, which is well suited to problems with several constraints that are potentially simultaneously active at convergence. The merit figure of the structural sizing step is blade cost, which is calculated from the SANDIA blade cost model. Gradients are computed by means of forward finite differences. Once the solver converges to a new blade structure, the process iterates back to the tuning of the LQR controller and all steps are repeated until blade cost converges to a pre-defined tolerance, which is usually set at 1%.

3 Comparison of design configurations

In this section, the baseline upwind model used as benchmark is first presented in Sect. 3.1. Then, Sect. 3.2 reviews the downwind design configurations developed from the baseline. These are finally compared in Sect. 3.3 in terms of loads, blade mass, blade cost, AEP and CoE. Finally, some critical aspects of the load aligned solution are discussed in Sect. 3.4.

3.1 Baseline model

The DTU 10 MW reference wind turbine (RWT) platform is here chosen as a significant test case. This wind turbine is a conceptual machine developed by the Wind Energy Department of Denmark Technical University (DTU), freely availably in the public domain for research purposes. The main characteristics of the wind turbine are reported in Table 1, while a more complete description of the model and the criteria used for its design are given in Bak et al. (2013). In this study, the blade prebend distribution is optimized with `Cp-Max` following Sartori et al. (2016), which resulted in the solution reported in Fig. 2. Given this prebend, the blade twist and internal structure are updated by the aerostructural design optimization described in Sect. 2.4, while keeping the planform shape unchanged. For simplicity, a reduced set of DLCs is used, which includes DLC 1.1, 1.3, 2.3 and 6.2. To reduce the computational cost, a single seed is used in the turbulent cases.

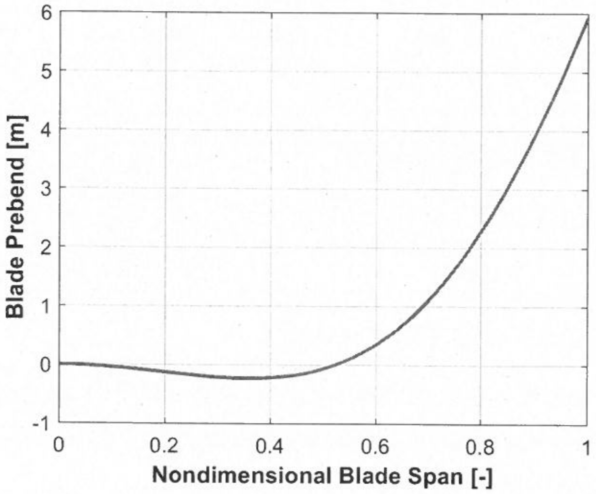

Figure 2. Prebend distribution obtained by `Cp-Max` during the re-design of the 10 MW DTU RWT.

Table 1. Main parameters of the DTU 10 MW RWT.

Data	Value
Wind class	IEC 1A
Rated electrical power	10 MW
Cut-in wind speed V_{in}	4 m/s
Cut-out wind speed V_{out}	25 m/s
Rotor diameter	178.3 m
Hub height	119.0 m

The blade inner configuration is a fairly standard spar box construction, except for the presence of a third shear web running along part of the blade span close to the trailing edge. Unidirectional fiberglass reinforcements are located at the leading and trailing edges, while an additional reinforcement is superimposed to the external shell in the blade root region. Table 2 reports the spanwise extension of the structural components and their materials. Transversely isotropic laminae are assumed to have the characteristics summarized in Table 2. The mechanical properties of the resulting composites are computed by classical laminate theory.

3.2 New configurations

The original upwind configuration (UW) is adopted as the starting point to establish a comparison among various alternatives:

a) UW5: upwind redesign with a 5% larger rotor diameter;

Table 2. Extent of the structural components and their materials in the blade of the 10 MW wind turbine.

Component	From (% η)	To (% η)	Material type	Longitudinal Young's modulus [MPa]	Transversal Young's modulus [MPa]	Shear modulus [MPa]
Spar caps	1	99.8	Uni-dir. GFRP	41,630	14,930	5,047
LE-TE reinforcements	10	95				
Root reinforcement	0	45				
First and second shear webs skin	5	99.8	Bi-axial GFRP	13,920	13,920	11,500
External shell	0	100	Tri-axial GFRP	21,790	14,670	9,413
Third shear web skin	22	95				
Shell and webs core	5	99.8	Balsa	50	50	150

b) DW: downwind design;

c) DW5: downwind redesign with a 5% larger rotor diameter;

d) DW5LA: downwind redesign with active load alignment and a 5% larger rotor diameter.

From a multi-body modeling point of view, configurations UW, UW5, DW and DW5 have exactly the same topological structure, where the only differences lay in the orientation of the rotor and in the tower shadow models. DW5LA uses instead the active coning solution based on actuated flap hinges, as discussed in Sect. 2.3.

Regarding DW5LA, it was observed that out-of-plane blade root moments cannot be reduced to zero, as this would require a flap angle γ in excess of 45 deg at rated wind speed. This would lead to a dramatic reduction of the rotor swept area and, consequently, of the generated AEP. After several tests, it was decided to limit the out-of-plane moment at blade root to 50% of the maximum steady state value measured in the UW design, namely 22 MNm. The resulting scheduled values of γ are reported in Fig. 3a, where the angle magnitude is visibly influenced by F_t. Between V_{in} and V_{r}, the prescribed γ is first held at 0 deg, since the out-of-plane moment at blade root is below the threshold of 22 MNm. Above a wind speed of 9 m/s, the prescribed γ rapidly increases until rated conditions following the increase in F_t, but keeping the out-of-plane moment at blade root below 22 MNm. Above V_{r}, blades are pitched into the wind, which results into a reduction of F_t and, consequently, also of γ.

Tests were also conducted to determine a suitable choice for the coning rate. Different values of $\dot{\gamma}$ from 0.001 deg/s to 1 deg/s were tested in DLC 1.1, analyzing the resulting out-of-plane blade root moment, as reported in Fig. 3b. Although lower values of $\dot{\gamma}$ could also probably be sufficient, a minimum of the loads is identified at 0.25 deg/s, which is the value used for the DW5LA design.

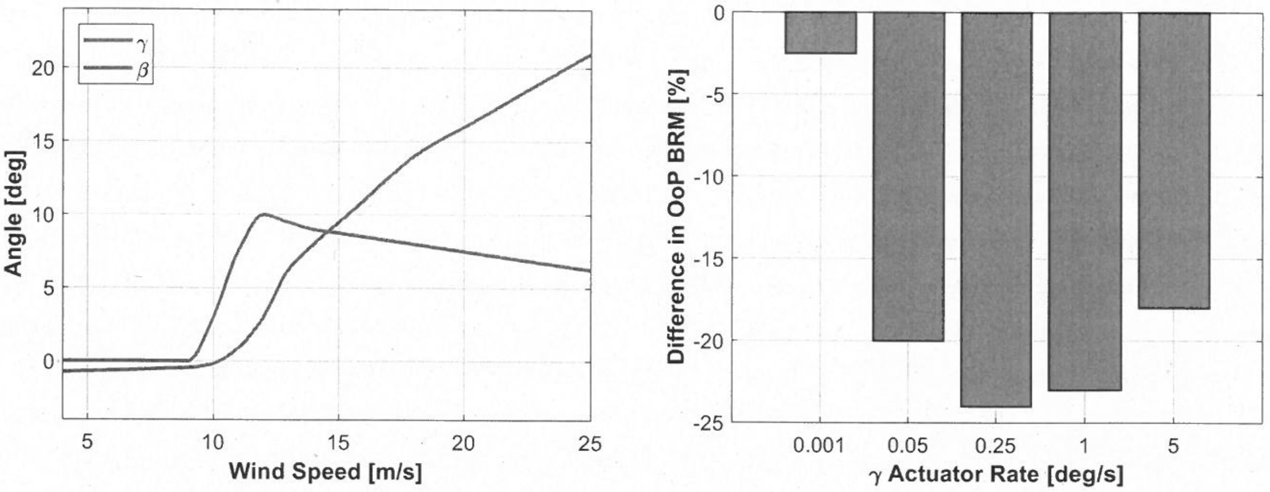

(a) Cone γ and pitch β angles vs. wind speed for DW5LA.

(b) Effect of γ rate on maximum out-of-plane moment measured at blade root in DLC 1.1.

Figure 3. Cone and cone rate for the DW5LA design.

All five configurations are then subjected to an aerodynamic optimization of the twist and a blade structural optimization, as described in Sect. 2.4. Once the two loops converge, the AEP and the CoE are evaluated. The comparison in terms of cost and performance is discussed next.

3.3 Cost and performance comparison

A comparison among the five configurations is presented with the histogram shown in Fig. 4a. First, as already observed in Bortolotti et al. (2016), the current cost models predict a reduction of CoE when the rotor is enlarged. Within this trend, downwind configurations appear to be able to successfully limit the growth in blade mass and cost. This effect is generated by the relaxed tower clearance constraint, which is instead a critical design driver for the UW and UW5 designs. It is however interesting to highlight that, although smaller than in the upwind cases, high blade deflections also occur in DW and DW5 during the emergency shutdowns simulated with DLC 2.3. Possibly, optimized shut down maneuvers could help in generating further mass and cost reductions, but a dedicated study would be needed to more precisely quantify any saving. Although costs are reduced, DW and DW5 generate smaller values of AEP compared to UW and UW5. These reductions are mostly caused by an increased flexibility of the blades, which bend when loaded, in turn reducing the rotor swept area. For a given rotor cone angle, this effect is more detrimental for downwind rotors compared to an equivalent upwind one, as cone and prebend are against the wind in the latter case. The comparison is instead different as soon as an upflow is present in the incoming wind, which is the typical case of complex terrain conditions when the turbine is located on a hill or close to a ridge. In the present

②

case, an upflow of 5 deg induces an increase in AEP of 0.7%, which is directly converted into a reduction of CoE. In this scenario, DW5LA not only has a lower blade mass and cost compared to UW5 and DW5, but also a higher AEP.

A load assessment is conducted looking at key ultimate and fatigue loads measured at blade root and at the hub. The comparison is reported in Fig. 4b. In terms of flapwise blade root moments (FBRM), downwind configurations help in reducing both ultimate and fatigue loads, with DW5LA achieving the best results. For edgewise blade root moment (EBRM), fatigue loads follow the blade mass trend. On the other hand, a growth is observed in DW5LA in the case of torsional blade root moments (TBRM) due to the increased blade out-of-plane deformations induced by a decreased blade stiffness. Finally, at the hub trends are more scattered, with a decrease of the ultimate thrust (ThH) for DW and DW5LA and an overall marked increase of ultimate out-of-plane bending moments (OoPMH), especially for DW5LA. Overall, DW and DW5 are associated with lower loading compared to UW and UW5, except for maximum OoPMH, which is generated during an emergency shut-down. DW5LA is instead effective in reducing FBRM and EBRM, but at the cost of increased torsional moments on the blades (which would impact the pitch system design), and out-of-plane moments at the hub (which would impact the design of the shaft and of the main bearings). A specific, more detailed, design ③ acitvity would be necessary to quantify these effects. In addition, DW5LA is prone to several critical aspects, which are assessed in Sect. 3.4.

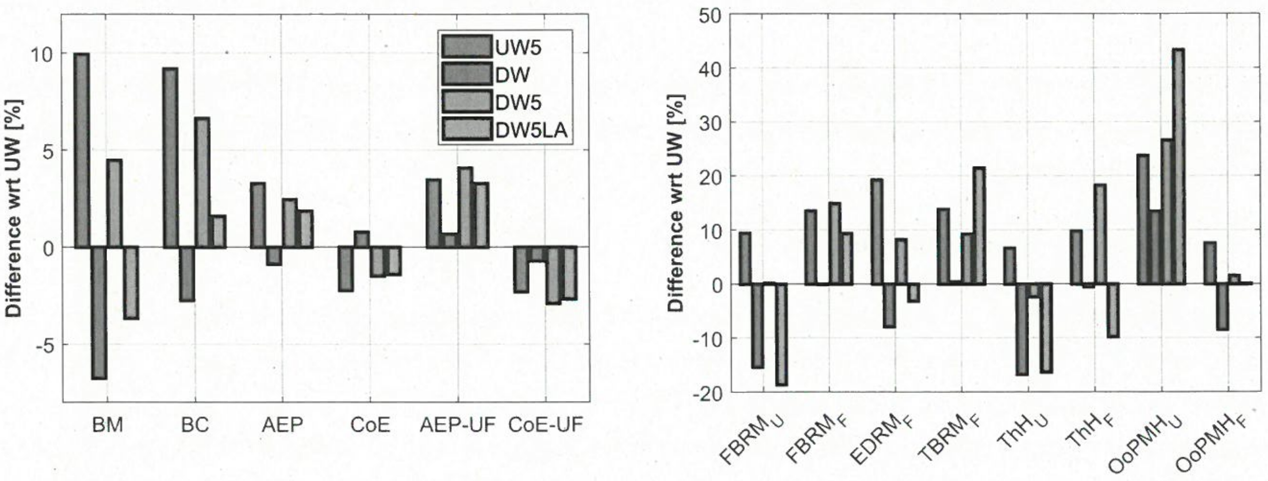

(a) Comparison in terms of blade mass (BM), blade cost (BC), AEP and CoE with 0 deg and 5 deg of upflow (UF).

(b) Comparison in terms of ultimate (subscript $(\cdot)_{\mathrm{U}}$) and fatigue (subscript $(\cdot)_{\mathrm{F}}$) loads for flapwise, edgewise and torsional blade root moments (FBRM, EBRM, TBRM) as well as thrust and out-of-plane moment at the hub (ThH and OoPMH).

Figure 4. Comparison in terms of main figures of merit (left) and loads (right) for the four designs with respect to the baseline configuration UW. The CoE of DW5LA does not include in the calculations the capital cost and power consumption of the active coning system.

3.4 Critical aspects of DW5LA and comparison with the literature

As shown in Fig. 5a, compared to configuration DW5, power losses of the design solution DW5LA are limited to wind speeds around rated conditions. However, active load alignment in turbulent dynamic cases is only partially effective. In fact, although blade root moments do indeed decrease thanks to active coning, moments at other points along the blade span are not significantly affected. It is speculated that a reduction of moments throughout a larger portion of blade span would necessitate of a truly morphing solution, with adjustable prebend. As a result of the only partial effectiveness of active coning, the blade cost of DW5LA is not significantly reduced compared to the one of configuration DW5. In addition, loads generated during storm conditions are not necessarily alleviated by active coning. In fact, folding the rotor will reduce its swept area, but it will also dramatically move the rotor center of gravity away from the tower, resulting in very large loading of the structure and foundations. For example, aeroelastic simulations were performed in storm conditions with a wind misaligned by ±30 deg, having folded the blades with a value of $\gamma = 60$ deg. Although a more sophisticated CFD analysis would be needed to accurately predict aerodynamic forces at such angles of attack, bending moments at the hub were doubled, while tower base moments increase by 40%.

Finally, for the chosen coning rate $\dot{\gamma}$ the actuators of configuration DW5LA have a non negligible power consumption. Figure 5b shows the consumption estimated during DLC 1.1 for the case without a power recovery system (label woRec) and with a recovery system having an efficiency of 80% (label wRec). Such solution, although technologically complex, would be able to recover most of the energy used by the actuators.

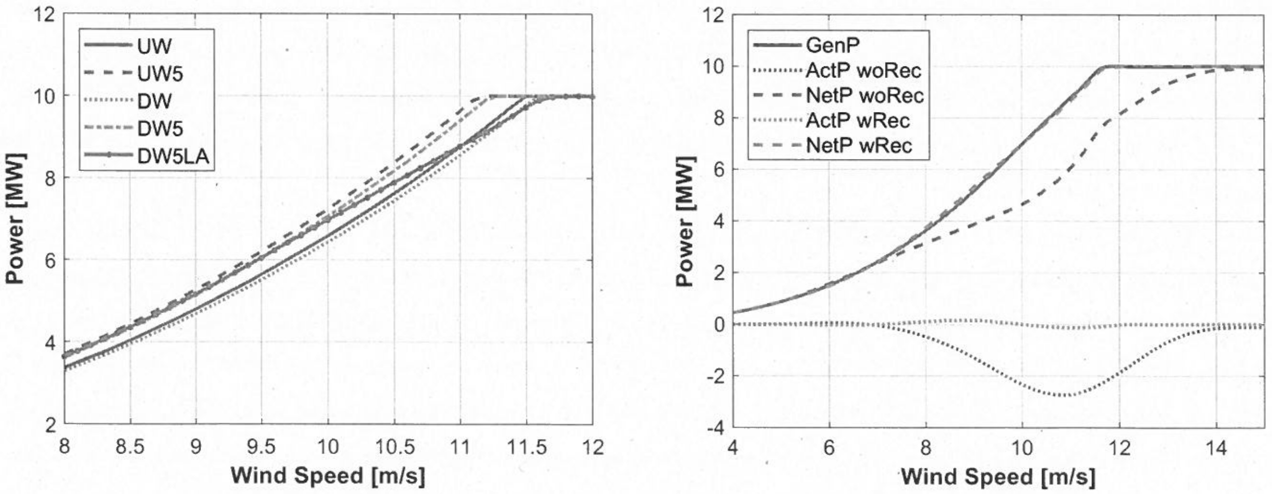

(a) Comparison of power curves.

(b) Power curves for DW5LA.

Figure 5. Power generation for the five designs (left) and power consumption of the three coning actuators with and without recovery system (wRec and woRec, respectively). The efficiency of the recovery system is assumed to be equal to 80%.

Overall, given the fact that the joints and actuators necessary for active coning would certainly pose serious engineering challenges and associated costs, a conventional downwind configuration would appear here to be more interesting than an actively load-aligned one. This conclusion is somewhat less promising than the ones presented in Ichter et al. (2016); Loth et al. (2017); Noyes et al. (2018). Two aspects may explain these differences. First, simplified analyses were conducted in the cited references, using steady-state conditions and no shut-down nor storm load cases, performing only a preliminary structural analysis. Secondly, the results presented in the literature adopt different design assumptions, including a two-bladed rotor with a constant γ (set to 17.5 deg). In this work, the use of a constant γ was attempted, but proved to be ineffective for the current 10 MW case because of a dramatic reduction in AEP and of a limited load alignment capability. In addition, a sufficiently high value of the coning rate appears to be necessary in highly turbulent wind conditions, such as the ones of the class 1A DTU 10 MW RWT considered here. These design choices differ from the ones assumed in the literature and, together with the arbitrary setting of the maximum blade root moment to 22 MNm, may affect the conclusions.

4 Conclusions and future work

This paper has presented a comparative study among five three-bladed upwind and downwind wind turbine configurations, with the aim of investigating the potential merit of downwind solutions and active load alignment in a 10 MW case. Based on the results reported herein, the following main conclusions can be drawn.

First, downwind rotors help in limiting mass and cost of very large blades. Specifically, results indicate reductions of 6% in mass and 2% in cost. It is speculated that further benefits could be obtained by optimized ad-hoc shut-down strategies. In addition, when the atmospheric flow is characterized by an upflow, such as in some complex terrain conditions, downwind machines generate a higher AEP than equivalent upwind designs because of a more favorable attitude of the rotor with respect to the incoming wind. In this study, a downwind rotor operating in a wind with an upflow of 5 deg generates 0.7% more AEP than an equivalent upwind configuration. Any such increase, together with savings in blade cost, can lead to CoE reductions at approximately the same loading.

Secondly, generating an effective load alignment in highly turbulent wind conditions, storms and faults appears to be a non-trivial task. In addition, losses in AEP compared to traditional downwind designs are observed. These effects negatively impact the CoE. The power consumed by the three coning actuators is also non negligible, peaking for the configuration analyzed here at a staggering average of nearly 3 MW around rated wind speed. Without a power recovery system, this would dramatically impact the AEP. The extra investment for the three actuators, both in terms of capital and operational cost, is also expected to significantly impact the CoE. Finally, during storms, the usefulness of load alignment is very questionable, as the folding of a large rotor is unrealistic due to the resulting dramatic increase of hub and tower base moments.

Overall, conventional (non-coning) downwind designs are found to be more promising. These configurations could offer advantages either in conditions of marked atmospheric upflow or in case of very large offshore machines, where blade mass needs to be limited. Having said this, it should also be remarked that the standard upwind solution appears to be very difficult to beat, even at these large machine sizes. Given the large body of knowledge and experience on this configuration accumulated by industry so far, it remains to be seen whether the advantages of downwind solutions are worth the effort and risk that are undoubtedly necessary to bring them to full maturity.

Additional investigations are necessary to address the assumptions and design decisions that may affect the conclusions of this work. For the comparison among UW, UW5, DW and DW5, an assessment of the effects of the four rotors on the design of the tower and of the nacelle components should be conducted. In addition, the blockage effect generated by the nacelle, which is not included in the present analysis, could possibly slightly improve the AEP and CoE of the downwind configurations. In this context, it would be useful to develop analytical corrections for BEM-based models to account for the presence of the nacelle in a downwind rotor. In terms of DW5LA, additional studies should assess the optimality of the design assumptions made so far, focusing especially on the amount of blade prebend, on the maximum flapwise blade root moment and on the coning rate. Finally, a more complete comparison with the existing literature should also consider the development of a teetering two-bladed downwind rotor, which was not studied here and might significantly change the conclusions.

Acknowledgements. The authors gratefully acknowledge the partial financial support of the ICER TUM-NTU project, directed by Prof. Subodh Mhaisalkar and Prof. Thomas Hamacher.

References

Badyda K, Dylik M. Analysis of the Impact of Wind on Electricity Prices Based on Selected European Countries. *Energy Procedia*, 2017;105:55-61. doi: 10.1016/j.egypro.2017.03.279

Bak C, Zahle F, Bitsche R, Kim T, Yde A, Henriksen LC, Andersen PB, Natarajan A, Hansen MH. Description of the DTU 10 MW reference wind turbine. *DTU Wind Energy Report-I-0092*, July, 2013.

Bauchau OA. Flexible Multibody Dynamics. Mechanics and Its Applications. *Springer*, 2011. ISBN: 978-94-007-0335-3

Bortolotti P, Bottasso CL, Croce A. Combined preliminary-detailed design of wind turbines. *Wind Energy Science*, 2016;1(1):71-88. doi: 10.5194/wes-1-71-2016

Bortolotti P, Sartori L, Croce A, Bottasso CL. Integration of multiple passive load mitigation technologies by automated design optimization - The case study of a medium-size onshore wind turbine. *Wind Energy*, Under Review, 2017.

Bottasso CL, Croce A, Savini B, Sirchi W, Trainelli L. Aero-servo-elastic modeling and control of wind turbines using finite-element multibody procedures. *Multibody System Dynamics*, 2006;16(3):291-308. doi: 10.1007/s11044-006-9027-1

Bottasso CL, Croce A, Nam Y, Riboldi CED. Power curve tracking in the presence of a tip speed constraint. *Journal of Renewable Energy*, 2012;40:1-12. doi: 10.1016/j.renene.2011.07.045

Bottasso CL, Bortolotti P, Croce A, Gualdoni, F. Integrated aero-structural optimization of wind turbine rotors. *Multibody System Dynamics*, 2016;38(4):317-344. doi: 10.1007/s11044-015-9488-1

Dykes K, Ning A, King R, Graf P, Scott G, Veers P. Sensitivity analysis of wind plant performance to key turbine design parameters: a systems engineering approach, *NREL/CP-5000-60920*, 2014.

Frau E, Kress C, Chokani N, Abhari RS. Comparison of Performance and Unsteady Loads of Multimegawatt Downwind and Upwind Turbines. *Journal of Solar Energy Engineering*, 2015;137(4):041004-041004-8. doi: 10.1115/1.4030314

Giavotto V, Borri M, Mantegazza P, Ghiringhelli G. Anisotropic beam theory and applications. *Computers & Structures*, 1983;16(1-4):403-413. doi: 10.1016/0045-7949(83)90179-7

Hansen MOL. Aerodynamics of Wind Turbines. *2nd edn. Earthscan, London*, 2008. ISBN: 978-1-84407-438-9

Ichter B, Steele A, Loth E, Moriarty P, Selig M. A morphing downwind-aligned rotor concept based on a 13-MW wind turbine. *Wind Energy*, 2016;19(4):625-637. doi: 10.1002/we.1855

INNWIND.EU, Deliverable 1.23, PI-based assessment of innovative concepts (methodology). INNWIND.EU technical report, Deliverable 1.23, April, 2014. Available at: www.innwind.eu

Johans W, Griffith DT. Large Blade Manufacturing Cost Studies Using the Sandia Blade Manufacturing Cost Tool and Sandia 100-meter Blades. *Sandia National Laboratories Technical Report*, 2013.

Janajreh I, Qudaih R, Talab I, Ghenai C. Aerodynamic flow simulation of wind turbine: Downwind versus upwind configuration. *Energy Conversion and Management*, 2010;51(8):1656-1663. doi: 10.1016/j.enconman.2009.12.013

Kress C, Chokani N, Abhari RS. Downwind wind turbine yaw stability and performance. *Renewable Energy*, 2015;83:1157-1165. doi: 10.1016/j.renene.2015.05.040

Kress C, Chokani N, Abhari RS. Design Considerations of Rotor Cone Angle for Downwind Wind Turbines. *ASME. J. Eng. Gas Turbines Power*, 2015;138(5):052602-052602-10. doi: 10.1115/1.4031604

Loth E, Steele A, Qin A, Ichter B, Selig MS, Moriarty P. Downwind pre-aligned rotors for extreme-scale wind turbines. *Wind Energy*, 2017;20(7):1241-1259. doi: 10.1002/we.2092

Noyes C, Qin C, Loth E. Pre-aligned downwind rotor for a 13.2 MW wind turbine. *Renewable Energy*, 2018;116(A):749-754. doi: 10.1016/j.renene.2017.10.019

Madsen HA, Johansen J, Sørensen NN, Larsen GC, Hansen MH. Simulation of Low frequency Noise from a Downwind Wind Turbine Rotor. *45th AIAA Aerospace Sciences Meeting and Exhibit*, Reno, Nevada, 2007. doi: 10.2514/6.2007-623

Manwell JF, McGowan JG, Rogers AL. Wind Energy Explained. *Wiley*, 2009. ISBN: 978-0-470-01500-1

Pitt DM, Peters DA. Theoretical prediction of dynamic inflow derivatives. *Vertica 5*, 1981;21-34

Peters DA, He CJ. Finite state induced flow models-part II: three-dimensional rotor disk. *J. Aircr.*, 1995;32:323-333. doi:10.2514/3.46719

Reiso M. The Tower Shadow Effect in Downwind Wind Turbines. *Ph.D. Thesis*, NTNU Norwegian University of Science and Technology, 2013.

Sartori L, Bortolotti P, Croce A, Bottasso CL. Integration of prebend optimization in a holistic wind turbine design tool. *Journal of Physics, Conference Series*, 2016;753. doi: 10.1088/1742-6596/753/6/062006

Soltani MN, Knudsen T, Svenstrup M, Wisniewski R, Brath P, Ortega R, and Johnson K. Estimation of rotor effective wind speed: a comparison. *IEEE T. Contr. Syst. T.*, 2013;21(4):1155–1167. doi:10.1109/TCST.2013.2260751

Wind Turbines Part 1: Design Requirements, Ed. 3. *International Standard IEC 61400-1*, 2005.

Zahle F, Tibaldi C, Pavese C, McWilliam MK, Blasques JPAA, Hansen MH. Design of an Aeroelastically Tailored 10 MW Wind Turbine Rotor. *Journal of Physics, Conference Series*, 2016;753. doi: 10.1088/1742-6596/753/6/062008

① Can you explain why this blockage effect is favourable, with respect to power/loads?

② How the AEP has been computed, how large is the uncertainty. 0.7% seems to be very small compared to the uncertainties in the calculation.

③ activity.

General comments.

① please describes in more details the assumption in the simulation study, for example the wind regime, turbulence intensity, wind shear

② How many seeds have been used to generate the turbulent inflow, is the number large enough to support the 0.7% AEP increase stated in the paper.

③ what kind of tower shadow model has been used for the down wind case.

④ how large is the uncertainties of the blade cost model of Sandia. Will the uncertainties increase when the model is used for 10 MW wind turbine blade, for which the cost model is not calibrated.

⑥ using active coning will introduce uncertainties in the cone angles, meaning each of the blades may have slightly different cone angle, How would that impact the loads.

⑥ what is the impact of down wind configuration ON the tower loads?

⑦ will pitch activities of down wind turbines increases tubulence?

⑧ complex terrain is not just an upflow angle, other flow characteristic may have also significant impacts. on the loads.